Molecular Crystals and Liquid Crystals
Publication details, including instructions for authors and subscription information:
http://www.tandfonline.com/loi/gmcl16

Studies of Cholesteryl Oleyl Carbonate in its Isotropic and Homeotropic States Using Optical Rotation, Kerr-Effect and Light-Scattering Techniques

M. S. Beevers [a], D. A. Elliott [a] & G. Williams [a]
[a] Edward Davies Chemical Laboratories, University College of Wales, Aberystwyth, Dyfed, SY23 1NE, U.K.

Version of record first published: 14 Oct 2011.

To cite this article: M. S. Beevers , D. A. Elliott & G. Williams (1982): Studies of Cholesteryl Oleyl Carbonate in its Isotropic and Homeotropic States Using Optical Rotation, Kerr-Effect and Light-Scattering Techniques, Molecular Crystals and Liquid Crystals, 80:1, 135-156

To link to this article: http://dx.doi.org/10.1080/00268948208071027

Mol. Cryst. Liq. Cryst., 1982, Vol. 80, pp. 135–156
0026-8941/82/8004-0135$06.50/0

Printed in the United States of America

Studies of Cholesteryl Oleyl Carbonate in its Isotropic and Homeotropic States Using Optical Rotation, Kerr-Effect and Light-Scattering Techniques

M. S. BEEVERS, D. A. ELLIOTT and G. WILLIAMS

Edward Davies Chemical Laboratories, University College of Wales, Aberystwyth, Dyfed, SY23 1NE, U.K.

(*Received May 21, 1981; in final form August 17, 1981*)

The temperature dependence of optical rotation, static and dynamic Kerr-effect, and polarized and depolarized dynamic light-scattering for cholesteryl oleyl carbonate has been studied in a range including the isotropic liquid, homeotropic, and supercooled homeotropic states. Above the isotropic-cholesteric liquid crystal transition, marked pre-transitional effects are observed and are interpreted in terms of the build-up of angular correlations between molecules. On supercooling through this transition the observed magnitudes and correlation times are continuous well into the supercooled region, but show a smaller variation with temperature than that observed in the pre-transition range due, apparently, to a tendency for the angular correlation factors to saturate at the lowest temperatures. These data are discussed in relation to mean-field theory for mesogens and to the nature of the phase transformations between isotropic liquid, homeotropic liquid, and cholesteric focal-conic liquid crystal states.

INTRODUCTION

Numerous studies have shown that liquid crystal-forming materials may exhibit pre-transitional behavior in their isotropic state at temperatures just above the transition: isotropic liquid → liquid crystal. The pre-transitional effects are most marked using techniques which are sensitive to the angular and spatial correlations between molecules, e.g., electro-optical Kerr-effect and quasi-elastic light-scattering. Studies using these techniques have been made for the nematogens MBBA,[1–5] alkyl cyanobiphenyls[6,7] and alkyl cyanophenylpyrimidines.[8] The observed properties (e.g. Kerr-constant) are a strong function of temperature and are usually analyzed using the Landau-de Gennes mean-field theory[9,10] in which it is proposed that the correlation

length $\xi(T)$ may be proportional to $(T - T^*)^{-\gamma}$ where γ is an unknown exponent and T^* is a temperature slightly below the transition point T_c for the transition isotropic liquid → nematic liquid crystal. For nematogens T^* is 0.1 to 1 K below T_c. Cholesteric mesogens have frequently been described as chiral-nematic mesogens because of similarities between the nematic and cholesteric phases. Cholesteric materials exhibit a complicated transition on heating and cooling. In the region of the overall transformation: cholesteric liquid crystal (focal-conic texture) ⇌ isotropic liquid, an intermediate state, called the "blue-phase" or "homeotropic-phase",[10-12] may occur. The formation of the blue-phase and its range of existence has been of considerable interest for a number of years.[10-24] At the outset of this work, it was our intention to study the Kerr-effect of a cholesteric material in its isotropic state in order to obtain information which would be complementary to that obtained for nematic-forming materials,[4,5-9] and hence would examine the applicability of the mean-field theory to a cholesteric material. We chose cholesteryl oleyl carbonate (COC) a material which had been studied earlier in this laboratory using dielectric techniques. It soon became apparent that the Kerr-effect measurements were complicated because COC, in common with other cholesteric materials, is optically active. It was therefore necessary to examine the theory of the measurement of the static and dynamic Kerr-effect of an optically active material and this was done by Beevers and Elliott[25,26] using a Jones-matrix representation of the electro-optical behavior of the material, in a manner very similar to that described by Watanabe.[27] During the course of our studies of the Kerr-effect and optical rotation ϕ for COC as a function of temperature, it became apparent that the material could be readily supercooled below the transition T(isotropic) → T(cholesteric focal-conic liquid crystal). This enabled us to extend the earlier studies of $\phi(T)$ for COC by Cheng and Meyer[28,29] who had examined the region above this transition. In addition we thought it desirable to study the quasi-elastic light-scattering behavior for our COC sample in the isotropic and supercooled states so that dynamic Kerr-effect and dynamic light-scattering data could be compared for the same material.

In view of the complicated nature of the transitions for cholesteric materials, our account makes extensive reference to earlier studies made using a variety of techniques for a number of materials. In order to establish a consistent nomenclature for the pattern of behavior, it is useful to summarize the transformations which occur on heating and cooling the isotropic liquid. Whilst there are a number of accounts describing different cholesteric materials we choose† to follow that given by Price and Wendorff[14a,b] which they

† Stegemeyer and Bergmann[15] have recently given a valuable account of the nature of the homeotropic phase, CT1, and its relation to phases I and CT_2. See also the Appendix of present paper for a discussion of the term T_c for cholesterics.

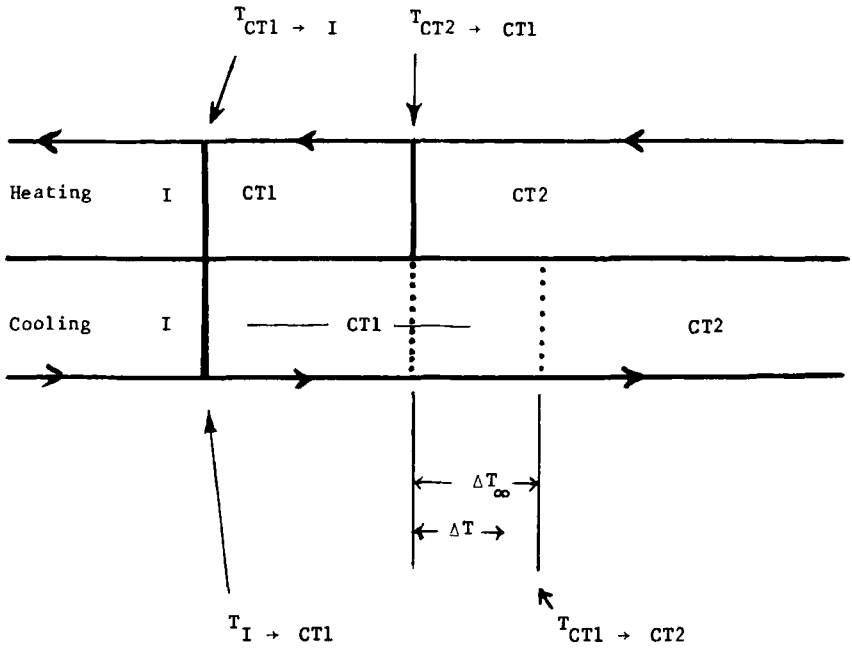

FIGURE 1 The phase transformations of a cholesteric mesogen on heating and cooling in the vicinity of the transformation from isotropic liquid (I) to cholesteric liquid crystal (focal-conic texture) CT2. Here CT1 denotes the "homeotropic" or "blue" phase, ΔT indicates the degree of supercooling of CT1 below the transition temperature $T_{CT2-CT1}$.

deduced for cholesteryl nonanoate. Figure 1 shows a diagram adapted from the scheme of Price and Wendorff as shown in their Figure 5 of Ref. 14b. On cooling the isotropic liquid (I), the material forms a "homeotropic" or "blue-phase" labelled CT1 at the temperature T_{I-CT1}. In the range T_{I-CT1} to $T_{CT2-CT1}$ the phase CT1 is stable but for $T_{CT1-CT2} < T < T_{CT2-CT1}$ the phase CT1 is metastable with respect to the "white-phase" or "focal-conic" cholesteric phase CT2. For cholesteryl nonanoate the range of supercooling ΔT_∞ may be as great as 8K. Ryumtsev and co-workers[13] showed that the effective time for the existence of the CT1 phase was strongly dependent upon the degree of supercooling, ΔT, being, for cholesteryl nonanoate, 8, 3, 1.5 and 0.2 hours for ΔT equal to 1, 2, 4 and 8K respectively, the process of transformation from CT1 → CT2 being a nucleated one. On heating the CT2 phase the material undergoes a sharp optical clearing point at $T_{CT2-CT1}$ and further increase in temperature gives the clear transparent isotropic liquid I at T_{CT1-I}. Thermodynamically there appear to be two phase transitions on heating. For example Armitage and Price[17] found that as the temperature is raised for the CT2 phase, there is a sudden change to CT1 at ~0.5K below the transition T_{CT2-I}. For cholesteryl chloride and for cholesteryl myristate and

$\Delta H_{CT1-I} \gg \Delta H_{CT2-CT1}$ and $\Delta V_{CT1-I} \gg \Delta V_{CT2-CT1}$; thus the transition CT2 → CT1, which is first-order, appears to involve only a slight reorganization of the material whilst that for CT1 → I is substantially greater. Very recently Armitage and Cox[21] studied the thermodynamic behavior of 4-(2′-methylbutylphenyl) 4′-(2″-methylbutyl)biphenyl-4-carboxylate in the range for the transition from cholesteric liquid-crystal to isotropic liquid. A small sharp thermal peak was observed at 115.9°C ($\Delta H = 0.04$ J g^{-1}) and a larger, but broader process in the range 117.5–120°C, peaking at 118.7°C was observed on heating. A further smaller peak was observed at 116.9°C ($\Delta H \simeq 0.008$ J g^{-1}). These may be assigned as CT2 → CT1 at 115.9°C and CT1 → I at 118.7°C, so the range of the "blue-phase" CT1, being 2.8°C, is exceptionally large for this cholesteric material. According to Armitage and Cox[21] there are two "blue-phases" for this material, these being observed as 'BP1' for $115.9 < T < 116.9$°C and 'BP2' for $116.9° < T < 118.7$°C. One important feature of this work is that they suggest that whilst the transition CT2 → CT1 is sharp and first order, the breadth of the transition CTl → I implies that it is second-order. We note that the equilbrium density-*vs*-temperature plot for cholesteryl nonanoate[14] exhibits a reversible broad curve from the line for the CT2 phase to the line for the isotropic phase starting at 89°C and finishing at 91.6°C, whilst the transition temperatures are $T_{CT1-I} = 91.6$°C, $T_{CT2-CT1} = 90.5$°C. This implies that the first-order transition CT2 → CT1 was giving only a small volume change, but the transition CT1 → I occurs, on heating, over a *range* of ~2.0°C and is complete at T_{CT2-I}. Such a transition is similar to that observed recently by Armitage and Cox[21] and discussed above. We therefore suggest that in Figure 1, $T_{CT2-CT1}$ is a first-order thermodynamic transition—with only small changes of ΔH and ΔV being involved—and that in the range $T_{CT2-CT1} < T < T_{CT1-I}$, the CT1 phase is stable but has a structure which changes rapidly with increasing temperature such that at T_{CT1-I} the structure is destroyed to the point that at higher temperatures the material behaves as an isotropic liquid. This means that the transformation CT1 → I occurs continuously over a range of temperature, and is therefore not a first-order thermodynamic transition, and T_{CT1-I} represents a limiting temperature for the overall process CT1 → I.

We have thought it necessary to review these earlier works in order to rationalize the pattern of behavior shown in Figure 1 and, importantly, to set the stage for the following account of our observations.

EXPERIMENTAL

The sample of COC supplied by Eastman-Kodak Ltd and was the same material as that used earlier[30] for dielectric, infra-red and refractive index meas-

urements. No further purification was made, except for light-scattering studies, where the material was filtered through a Millipore filter. The sample in the CT2 form exhibited an optical clearing point at 307.8K, i.e. at $T_{CT2-CT1}$. We note that Gray and Hannant[31] recently discussed the formation of the crystalline solid and the mesophases of COC in relation to its purity. They give $T_c = 307.2$K, determined by optical microscopy, for their analytical sample.† We found that the sample of COC was readily supercooled from isotropic to the CT1 phase below $T_{CT2-CT1}$, and behaved thermally in a manner in accord with the above account of Figure 1.

The apparatus used for our Kerr-effect measurements has been described previously.[32-34] As mentioned above, COC, in common with other cholesteric materials, is optically active and shows a strong dependence of the optical activity coefficient with temperature. The Kerr-constants were measured using the "pulsed-null" and "DC-null" methods which normally yield $(\delta/4)$ and $(\delta/2)$ respectively. δ is the phase-retardation of the sample. For COC the correction factors calculated by Beevers and Elliott[25,26] were applied where necessary. The dynamic Kerr-effect measurements were made using the quadratic detection method for which, in the case of a non-optically active material, the intensity of light transmitted by the analyzer is proportional to $\sin^2(\delta/2)$. For an optically-active material, provided that $0 < \delta < 50°$, and $0 < \phi < 50°$, this law is also obeyed.[25,26] For the present studies we operated in the ranges $0 < \delta < 25°$ and $0 < \phi < 20°$ and therefore no significant correction factors[25,26] were required. The transients were recorded using a Datalab DL.920 transient recorder and were transferred to paper tape for subsequent processing on an ICL 4130 computer. The Kerr-cell was 5.0 cm long with an interelectrode spacing of 1 mm. The sample was controlled to ± 0.005 K using a specially designed control unit[25] and all measurements were made using a He/Ne laser with polarized radiation operated at 632.8 nm.

The light-scattering measurements were made at R.S.R.E. Malvern using a Malvern Precision Instrument 96-channel correlator together with a Coherent Radiation Krypton laser operated at 647.1 nm. The intensity of scattered light and the intensity-intensity correlation function $g_2(t)$ was measured for polarized (VV) and depolarized (VH) scattering. The amplitude-amplitude correlation function $g_1(t)$ was calculated in the usual manner.[35,36] The sample was contained in a 1 cm^3 cuvette which was immersed in a water bath controlled to ± 0.005 K using a Eurotherm unit. The optical rotation data were obtained as a part of both the Kerr-effect and light scattering data and the values to be given below refer to the He/Ne line.

† T_c is T_{CT1-I}, in our notation, for the data of Ref. 31. We thank the referee for drawing this to our attention.

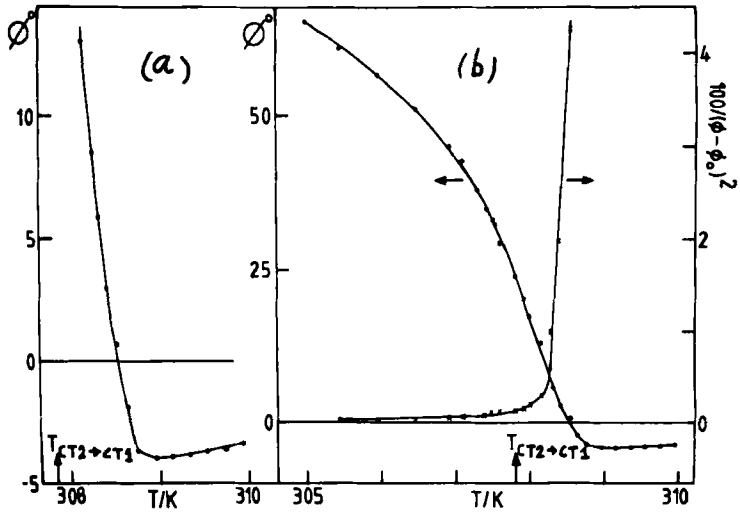

FIGURE 2 Optical rotation $\phi(T)$ for COC in (a) the pre-transition region (b) in the pre-transition and supercooled regions. Also shown in (b) is $[\phi(T) - \phi_0(T)]^{-2}$ against T/K.

RESULTS

Figure 2 shows plots of optical rotation $\phi(T)$ for 1 cm path length for COC in the pre-transition region (Figure 2a) and an extended range, which includes the pre-transition region and the supercooled range, for CT1 (Figure 2b). On heating this sample in steps of 0.1 K and waiting for temperature equilibration (20 min. per step) the transition $T_{CT2-CT1}$ was seen to occur sharply at 307.8 K, and was reproducible. Measurements of $\phi(T)$ below $T_{CT2-CT1}$ were achieved by cooling the isotropic liquid in steps of 0.1 K and allowing equilibration to occur (20 min. per step). $\phi(T)$ was found to be continuous and reversible through $T_{CT2-CT1}$, when the material was in its supercooled CT1 state. Crystallization of the supercooled phase CT1 to phase CT2 in the range 305 K $< T <$ 307.8 K occurred by a nucleated process, as is usual for cholesteric materials,[14-20] but on heating the phase CT2 to form CT1, the values of $\phi(T)$ for $T >$ 307.8 K fell exactly on the curve of $\phi(T)$ obtained on cooling from the isotropic phase. Thus the curve shown in Figure 2b is that connecting the isotropic phase and the homeotropic phase (CT1) in its stable and supercooled ranges. No discontinuities are evident in this curve. Our data shown in Figure 2a are similar in magnitude and functional form to those given by Cheng and Meyer.[28,29] The change in sign as temperature is decreased shows that the specific optical rotation for the molecules and for their chiral aggregates are of opposite sign. There is a discrepancy of about 11 K between the earlier data[28,29] and the present data whose origin is unclear. The sample used earlier may have been impure, leading to a lower $T_{CT2-CT1}$, but a value of 11 K seems

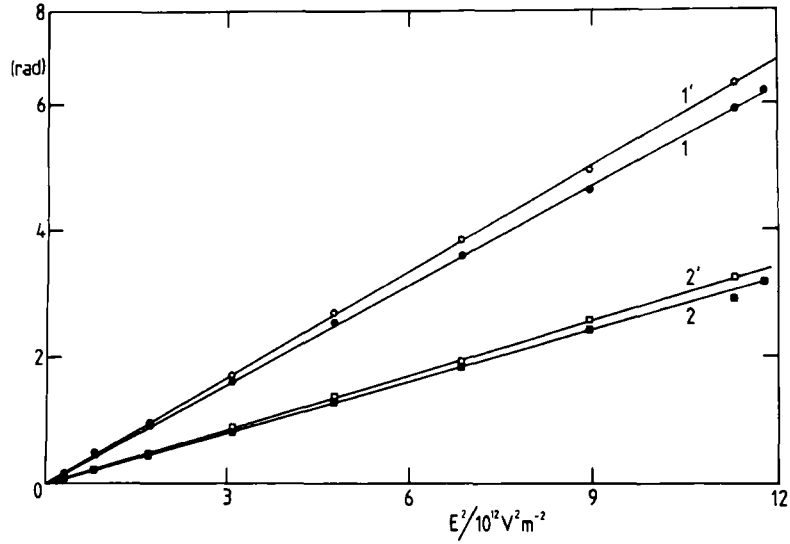

FIGURE 3 Angle of rotation (radian) of the analyzer against the square of the applied electric field for COC at 309.0 K. Lines 1 and 1' refer to uncorrected and corrected values of ($\delta/2$) obtained by the "DC" method, and lines 2 and 2' refer to uncorrected and corrected values of ($\delta/4$) obtained by the "pulsed-null" method.

unusually large. Included in our Figure 2b is a plot of $(\phi - \phi_0)^{-2}$ against T for comparison with the theoretical function $(\phi - \phi_0)^{-1} \propto (T - T^*)^{(1/2)}$ derived by Cheng and Meyer from the Landau-de Gennes theory. $\phi_0(T)$ is the optical rotation coefficient for individual molecules and values are estimated by extrapolation of the data in the range 309–310 K to lower temperatures. We find $\phi_0(305\text{ K}) = -6.4°\text{ cm}^{-1}$ varying to $\phi_0(310\text{ K}) = -3.1°\text{ cm}^{-1}$. The plot of $(\phi - \phi_0)^{-2}$ is curved at all temperatures, but a rough extrapolation of the high temperature line yields $T^* = 308.2$ K, a value exceeding $T_{CT2\text{-}CT1}$ for this sample and is thus inconsistent with mean field theory.

The function $[\phi(T) - \phi_0(T)]$ clearly does not follow a $(T - T^*)^{-\gamma}$ relation for COC† and therefore does not obey the Landau-de Gennes theory in this range. Of some significance is the observation that whilst $\phi(T)$ increases monotonically for $T < 308.5$ K, its slope reaches a maximum at $T \simeq 307.3$ K. Cheng and Meyer only report data above the clearing point $T_c = T_{CT2\text{-}CT1}$, but our extended data show that $\phi(T)$ varies continuously through T_c as we cool the isotropic liquid (or CT1) into the supercooled range.

The Kerr-effect could not be measured in the supercooled region since light-scattering effects obscure the field-induced birefringence. Figure 3 shows plots of the uncorrected and corrected angles of rotation of the analyzing prism at

† Note that Cheng and Meyer found that dextro-rotatory EBMBA followed this relation with $\gamma = 0.498$.

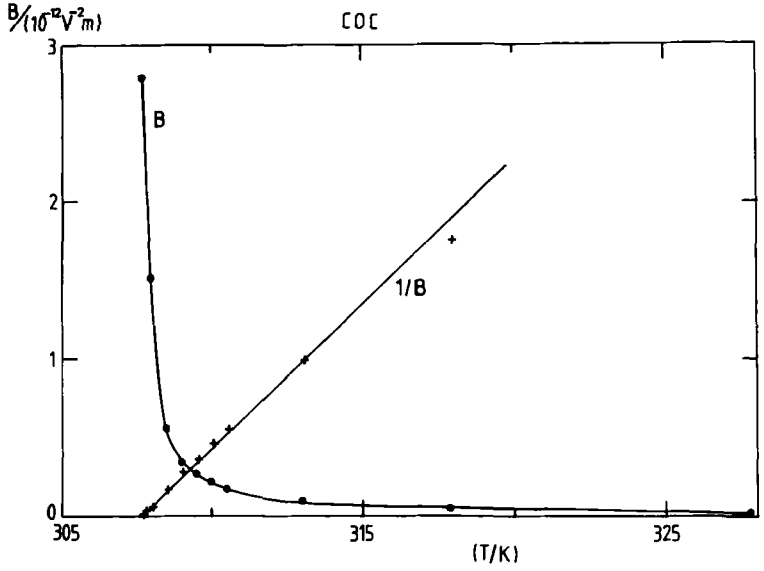

FIGURE 4 Static Kerr-constant B and its reciprocal plotted against temperature for COC.

309 K as a function of E^2 for the two methods employed. From a series of such measurements, the Kerr-constant $B(T) = \delta(T)/(lE^2)$, where δ, l and E are phase retardation, cell-length, and electric field respectively, was measured and Figure 4 shows $B(T)$ in the range 305–325 K. Pre-transitional behavior similar to that observed for nematogens[3-8] is evident and the plot $[B(T)]^{-1}$ also shown in the figure is approximately linear, given $T^* = 307.4$ K. At the lowest temperatures studied a small permanent birefringence was observed in the absence of an applied field whose value increased with decreasing temperature.

Figure 5 shows the Kerr-effect rise and decay transients obtained using quadratic detection at 309.0 K. Such data were fitted using the empirical relaxation function of Williams and Watts.[37,38]

$$\psi(t) = \exp - (t/\tau)^{\beta} \qquad (1)$$

Figure 6 shows the plot $\ln [- \ln [1 - \psi_{K,r}(t)]]$ against $\ln (t/\tau_{K,r})$ for the rise transient of Figure 5. The figure also shows the line calculated for $\beta = 0.92$ and $\tau_{K,r} = 41$ μs and a reasonable fit is obtained to the observed transient. Figures 7 and 8 show observed and calculated plots for the decay transient at 309.0 K with $\tau_{K,d} = 41$ μs and $\beta = 1.1$. This value of β is sufficiently close to unity to suggest that this process obeys a single exponential decay function. At lower temperatures, it was not possible to extinguish the transmitted light by rotation of the analyzer, but a position of minimum intensity was readily found. This position was used for the dynamic measurements. In order to in-

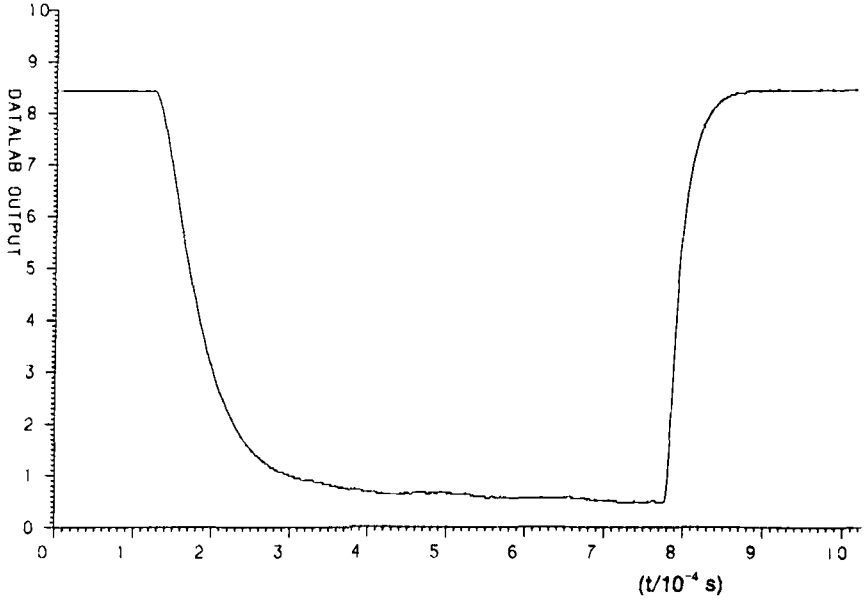

FIGURE 5 Kerr-effect rise and decay transients for light intensity·COC at 309.0 K and $E = 2.4 \times 10^6$ Vm^{-1}, obtained in quadratic detection.

vestigate the behavior, a ($\lambda/4$) plate was placed between Kerr-cell and analyzer and the mutual orientation of this plate and the analyzer was adjusted for minimum intensity of transmitted light. This was substantially less than the minimum value obtained in the absence of the ($\lambda/4$) plate, indicating that the material is birefringent in the absence of E for temperatures approaching T_c. The residual retardation angle, δ_0, was measured as the change of the analyzer position for minimum transmitted light with and without the ($\lambda/4$) plate. δ_0 increased from 0 to 10^2mrad as T was decreased in our range of observation. The Kerr-effect transients at the lower temperatures were affected by the residual birefringence. When the electric field was applied as a rectangular function the intensity of the transmitted light $I(t)$ followed the form shown in Figure 9 for quadratic detection at 307.7 K. When E is applied as a step, $I(t)$ first decreases and then increases with time. When E is removed as a step, the transient $I(t)$ decreases to the level obtained for the step-on transient and then gradually returns to a steady value. Such data were analyzed for the step-off transients by the relation

$$I(t) = I_s + C \sin^2 [(\delta_0 + (\delta_{K,d}(t))/2] \quad (2)$$

I_s, C, and δ_0 are respectively, the intensity of scattered light, a proportionality factor, and the phase retardation in the absence of E. $\delta_{K,d}(t)$ is the Kerr-effect

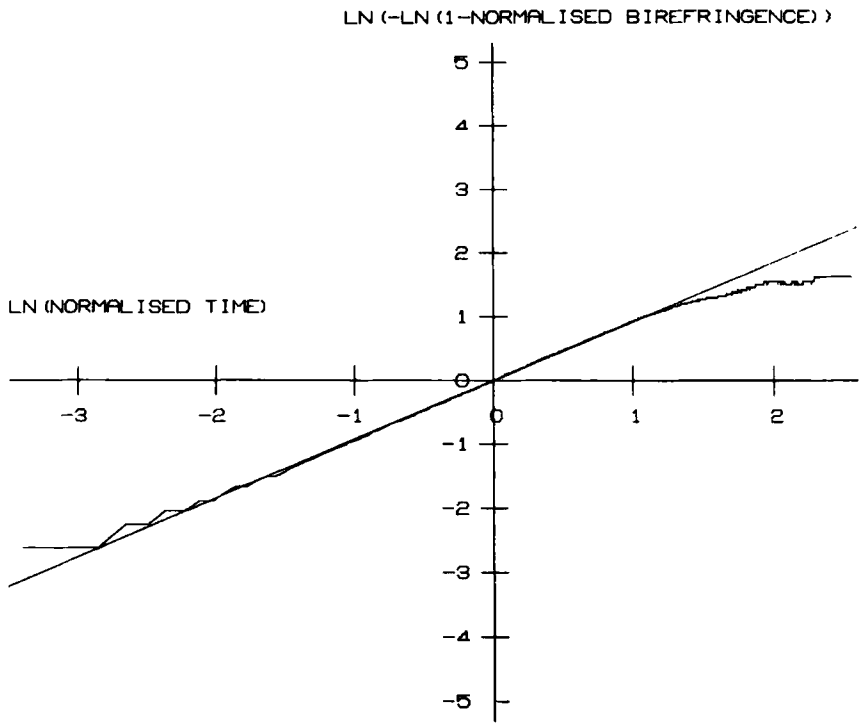

FIGURE 6 $\ln[-\ln(1-\psi_{K,r}(t)]$ against $\ln(t/\tau_{K,r})$ for COC at 309.0 K. The straight line is calculated for $\beta = 0.92$ and $\tau_{K,r} = 41\mu s$.

decay phase-retardation. An additional complication occurs for the rise transient. Figure 9 shows that the rise transient has a long-time "tail" and the derived Kerr-effect rise-transient is only poorly-fitted by Eq. 1 with $\beta_{K,r} \simeq 0.5$ and giving $\tau_{K,r} \gg \tau_{K,d}$. Since $\beta_{K,d} \simeq 1.0$ for the Kerr-effect decay transient, we consider that the differences between the Kerr-effect parameters for rise and decay transients are due to the inclusion of the slow tail of the rise transient. We suggest that this slow tail is due to heating of the sample in the presence of E. For normal materials heating effects would not appreciably affect ϕ or B, but for COC close to T_c both vary rapidly with temperature (Figures 2 and 4), so heating upsets the extinction condition for the analyzer and leads to the observed increase in $I(t)$ as a long time tail.

The values of τ and β for Kerr-effect rise and decay transients are summarized in Table I. For the decay transients, near single relaxation time behavior is observed at all temperatures. For the rise transients, $\beta_{K,r}$ obtained using Eq. 2 is near to single relaxation time behavior at higher temperatures, but falls at the two lower temperatures due to the artifact of the heating effects just

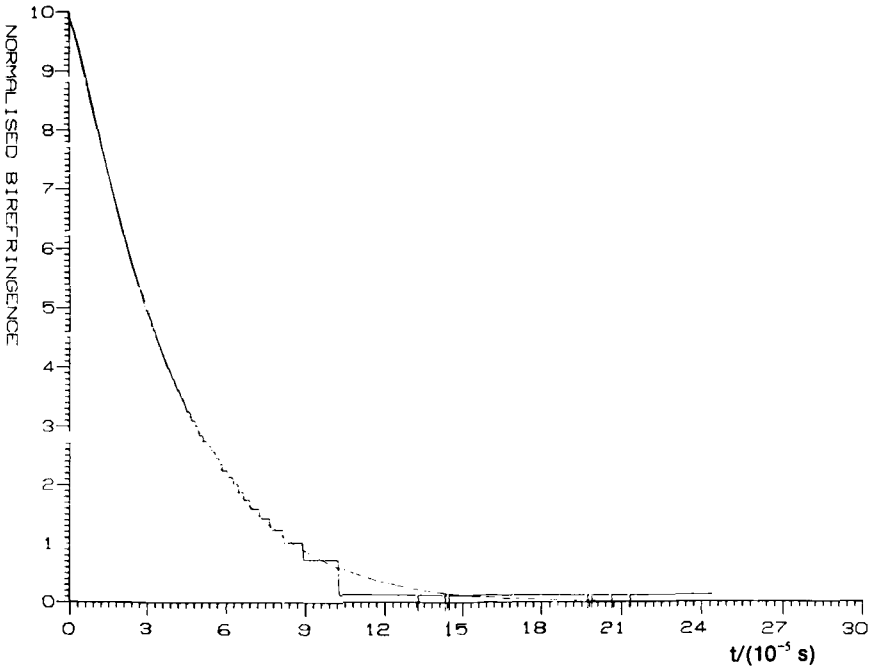

FIGURE 7 Observed and calculated normalized birefringence for the decay transient of COC at 309.0 K. The curve is calculated for $\beta = 1.1$ and $\tau_{K,d} = 41\mu s$.

described. If allowance is made for the long time tail, $\beta_{K,r}$ increases to unity and $\tau_{K,r}$ is slightly decreased from the values given in the Table. Thus $\tau_{K,r} \simeq \tau_{K,d}$ at all temperatures and Figure 10 shows log τ(Kerr) against temperature. As temperature decreases τ(Kerr) increases rapidly.

The intensity of polarized scattered light, I_{VV}, and depolarized scattered light, I_{VH}, are shown as a function of temperature in Figure 11. The correlation functions $g_1(t)$ for polarized (VV) and depolarized (VH) scattering could not be fitted by single-relaxation time functions, so the Williams-Watts equation (Eq. 1) was again employed. Table II shows the derived values of τ and β. As temperature decreases, the departure from single relaxation-time behavior becomes increasingly apparent. A considerable time elapsed between the Kerr-effect and dynamic light scattering experiments. However, it was found that the $\phi(T)$ data obtained for each experiment could be accurately superposed by moving the Kerr-effect data 0.8 K to higher temperatures. In Figure 10, the values of τ(Kerr) have been shifted by this amount.

The angular dependence of the light scattering behavior was examined in a further study and results are summarized in Table III. At the two highest temperatures the values are essentially independent of scattering angle Θ with

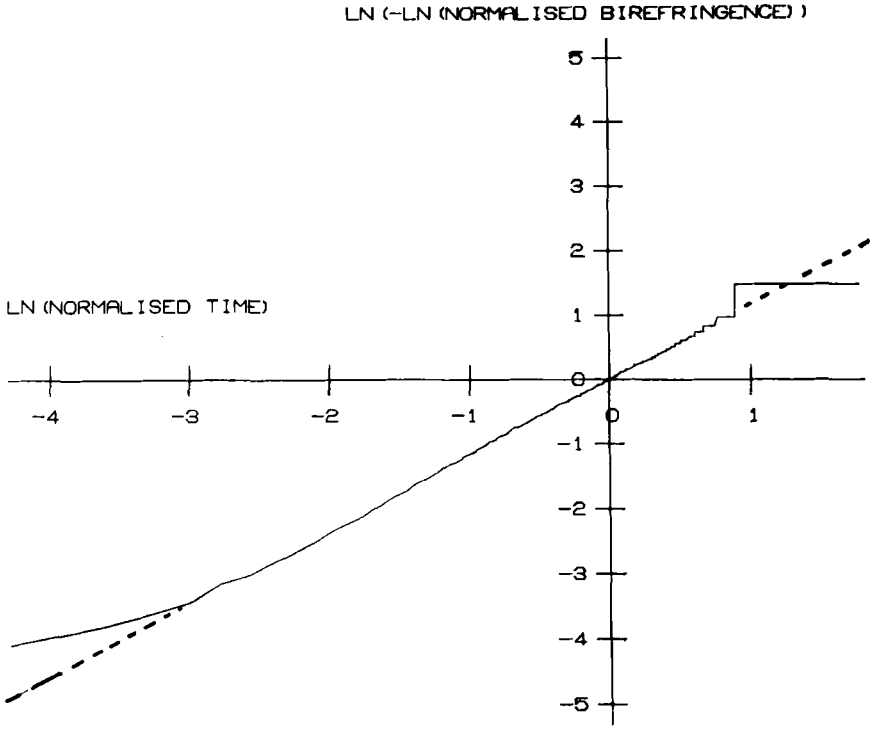

FIGURE 8 $\ln[-\ln \psi_{K,d}(t)]$ against $\ln(t/\tau_{K,d})$ for COC at 309.0 K. The straight line is calculated for $\beta = 1.1$ and $\tau_{K,d} = 41\mu s$.

single relaxation-time behavior being observed. However for the CT1 phase (the blue phase) at 307.4 and 305.6 K, τ increases with increasing Θ. Kerr-effect and light-scattering data should be compared at $\Theta \to 0$, but the data of Table III and Figure 10 show that the correction for comparison purposes is small in the range of overlap between the two studies.

DISCUSSION

In view of the apparent complexity of the phase behavior of COC and like mesogens, and the fact that we have used three techniques in this study, it seems desirable to organize our discussion in terms of (a) current thinking of the structures and dynamics in the isotropic and CT1 phases, (b) the information obtained from the individual techniques, and (c) the comparability of results.

First we note that the de Gennes theory[9,10] was used by Cheng and Meyer[28,29] to interpret $\phi(T)$ data for several cholesteric materials, including

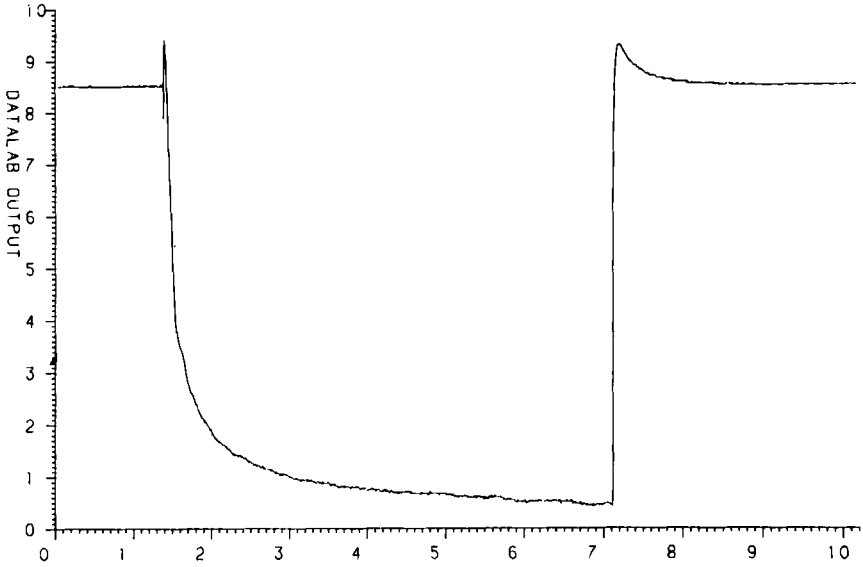

FIGURE 9 The Kerr-effect rise and decay transients for light intensity for COC at 307.7 K obtained in quadratic detection.

COC, for the isotropic liquid in its pre-transition region. The basis of the theory is to expand the free-energy density in terms of a tensor order parameter $Q_{\alpha\beta}$ which, for uniaxial nematics, takes the form

$$Q_{\alpha\beta} = \text{diag}\ \{-Q/2, -Q/2, Q\} \tag{3}$$

where Q is a macroscopic order parameter. Hence the free energy density F_N for the nematogen is written as

$$F_N = F_0 + \tfrac{1}{2} A\ Q_{\alpha\beta}Q_{\beta\alpha} + \tfrac{1}{3} B\ Q_{\alpha\beta}Q_{\beta\gamma}Q_{\gamma\alpha} + \ldots . \tag{4}$$

$A(T)$ is assumed to have the form

$$A(T) = a(T)\ (T - T^*)^{-\gamma} \tag{5}$$

TABLE I

Dynamic Kerr-effect data for COC

T/K	$E/(10^{-6}\ \text{Vm}^{-1})$	$\tau_{K,r}/(\mu s)$	$\beta_{K,r}$	$\tau_{K,d}/(\mu s)$	$\beta_{K,d}$
309.01	1.4	44	1.00	43	1.05
309.01	2.45	41	0.92	41	1.14
308.49	1.05	72	0.93	69	0.97
308.00	1.14	300	0.70	220	0.92
307.74	0.877	1000	0.64	970	0.95

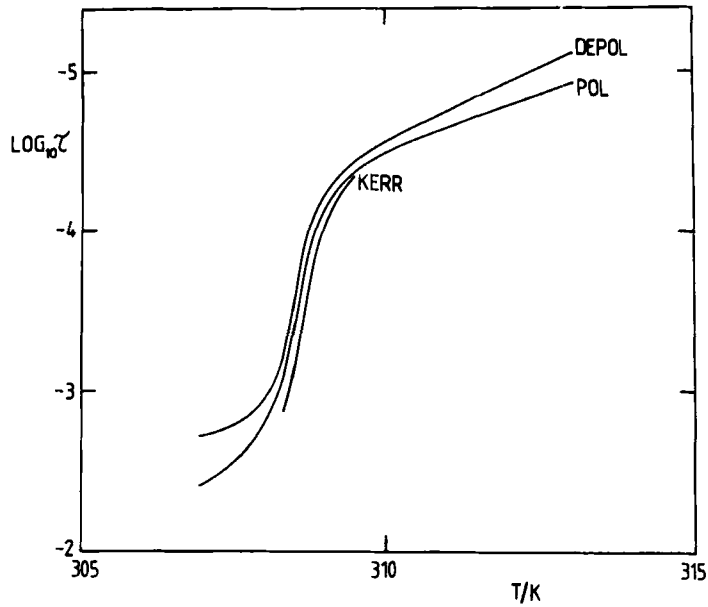

FIGURE 10 Plots of the logarithm of $\tau_{K,r} \simeq \tau_{K,d}$, τ_{VV} and τ_{VH} against temperature for COC.

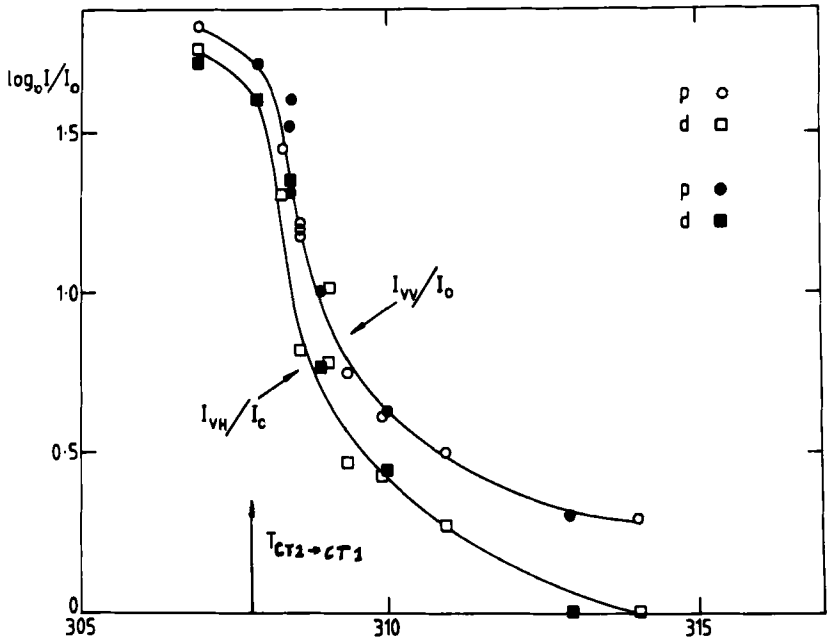

FIGURE 11 Plots of the logarithm of (I_{VV}/I_0) and (I_{VH}/I_0) against temperature for COC. Data from two runs are shown as (○ and ●) and (□ and ■) for polarized and depolarized scattering respectively. I_0 is a reference level measured at 314 K.

TABLE II

Dynamic Light Scattering Data for COC

T/K	Polarized $\tau_{VV}/\mu s$	Polarized β_{VV}	Depolarized $\tau_{VH}/\mu s$	Depolarized β_{VH}
313.05	11 ± 1	0.92 ± 0.05	7	0.9 ± 0.1
310.90	23.0 ± 0.5	0.87 ± 0.05	17.7 ± 0.5	0.95 ± 0.02
309.90	33.0 ± 0.8	0.93 ± 0.01	29 ± 2	0.92 ± 0.02
309.35	49.5 ± 0.5	0.95 ± 0.02	41 ± 1	0.93 ± 0.01
308.85	83 ± 1	0.92 ± 0.01	72 ± 1	0.92 ± 0.01
308.60	266 ± 15	0.78 ± 0.03	155 ± 2	0.85 ± 0.02
308.35	790 ± 10	0.68 ± 0.03	600 ± 50	0.68 ± 0.04
306.95	3900 ± 100	0.56 ± 0.03	1870	(0.8)

where $a(t)$ has only a weak temperature dependence,[9,10,28,29,39] γ is the unknown exponent, and T^* is an apparent second-order transition temperature. $T^* < T_{I\text{-}CTI}$, as was mentioned in the Introduction. The Q^3 and higher-order terms impose a first-order transition, preventing the observation of T^*. Cheng and Meyer[28,29] developed the above theory for cholesterics, adding a pseudoscalar term to F_N such that

$$F_C = F_N + \frac{27}{4} L_1 q_0^2 S^2 + \ldots \tag{6}$$

S is a microscopic order parameter (see Ref. 29 for the definitions of S and Q and their inter-relation) and q_0 is a quantity whose sign depends upon the nature of the chiral aggregate. L_1 is an elastic constant. de Gennes[9] suggests that

TABLE III

Light Scattering Data for COC (Experimental Run 3)

T/K	Angle/Degrees	$(\log_{10} I_{VV})$	$(\log_{10} I_{VH})$	$(\log_{10}\tau_{VV}/s)$	β_{VV}	$(\log_{10}\tau_{VH}/s)$	β_{VH}
309.85	90	1.29	—	−4.42	.76	—	—
309.85	153.7	1.58	—	−4.50	.91	—	—
309.2	63.7	1.44	1.34	−4.27	0.90	−4.44	0.91
309.2	90	1.37	1.29	−4.37	0.95	−4.45	0.87
309.2	116.3	—	1.30	—	—	−4.49	0.93
309.2	153.7	1.75	1.57	−4.28	0.95	−4.43	0.94
308.7	63.7	1.64	1.54	−4.04	0.90	−4.20	0.94
308.7	90	1.57	1.51	−4.08	0.90	−4.17	0.93
308.7	116.3	1.63	1.56	−4.12	0.94	−4.14	0.93
307.4	63.7	2.45	2.39	−2.82	0.69	−2.91	0.71
307.4	90	2.43	2.39	−2.72	0.69	−2.81	0.65
307.4	116.3	2.56	2.53	−2.53	0.64	−2.61	0.69
305.6	63.7	—	2.59	—	—	−2.72	0.71
305.6	90	2.62	2.71	−2.60	0.73	−2.54	0.71
305.6	116.3	—	2.75	—	—	−2.26	0.64

$(2\pi/q_0)$ is approximately equal to the pitch of the helix just above T_{CT2}. $T_{CT1} = T_C$. Cheng and Meyer derived the results that $(T_C - T^*)$ is equal to $(B S_C/6a)$ and $\{(B S_C/6a) - 9 L_1 q_0^2/a\}$ for nematic and cholesteric-forming materials respectively. $S_C = S(T_C)$. Thus the theory predicts a first-order transition for both types of mesogen, although the expressions for $(T_C - T^*)$ are only semi-quantitative, since truncation of F is only valid for $T > T_C$. The estimates of $(T_C - T^*)$ were smaller for cholesterics than for nematics so they suggested that the transition at T_C will become more second-order in nature for cholesterics. For cholesterogens, Cheng and Meyer predicted that $[\phi(T) - \phi_0(T)]$ would be proportional to $q_0\xi_1 \propto (T - T^*)^{-1/2}$ in the pre-transition region. According to de Gennes,[9,10] $q_0\xi_1(T_c) < 1$, and the helical pitch the isotropic phase would display just above T_c is $(2\pi/q_0)$. Since the optical rotation, ϕ, is proportional to $q_0\xi_1$, it follows that ϕ is non-singular near T_c[9,10]. de Gennes[9,10] also suggested that for a nematic material in its isotropic phase $q_0\xi_1 > \frac{1}{2}$ and hence a maximum intensity of scattered light $I_{xy}(q)$ should occur at $q = 0$. Here q is the wave-vector for scattered light. For a cholesteric material $q_0\xi_1(T)$ may be greater than $\frac{1}{2}$ with the consequence that a maximum in $I_{xy}(q)$ occurs for $q \simeq q_0$. This would lead to Bragg-scattering in the isotropic liquid reminiscent of Bragg-scattering in the liquid-crystal phase. Yang[39] denoted the temperature at which Bragg-like peaks are first observed as T_{BF}. He found that at T_{BF} the condition $q_0\xi_1(T_{BF}) \simeq 0.5$. For $T > T_{BF}$, Yang showed that the intensity I and the line-width Γ for scattered light should, according to mean-field theory, obey the relations

$$I_{ii}^{-1}(q) = A(T)\,[1 + \xi^2 q^2] \tag{7}$$

$$\Gamma = \frac{A}{\nu}(T)\,[1 + \xi^2 q^2]$$

where ii indicates laboratory coordinates, $\xi = (L_1/A)^{1/2}$, and ν is a factor having the dimensions of a viscosity. If the cholesteric material remains in its isotropic phase for $T > T_{BF}$ then $I_{xy}(q)$ is expected to have a complicated dependence upon q, given by[39]

$$I_{xy}(q) = \frac{1}{A}(T)\,\frac{1 + \xi^2 q^2}{1 + \xi^2 q^2 - 4q_0^2 q^2 \xi^4} \tag{8}$$

and Bragg-like interference will be observed. Such is the current approach to the pre-transitional behavior of cholesteric liquid-crystal-forming materials.

Cheng and Meyer[28,29] had shown that $\phi(T)$ exhibited pre-transitional behavior for COC, cholesteryl 2-(2-ethoxyethoxy)ethyl carbonate (CEEEC) and *p*-ethoxybenzal-*p'*-(β-methylbutyl)aniline (EBMBA), and they had fitted the $[\phi(T) - \phi_0(T)]$ data for EBMBA to the function $(T - T^*)^{-0.5}$ with $T^* = T_C - 0.42$ K. Thus, whilst the optical rotation of COC was not demonstrated

to conform with the Landau-de Gennes theory, that for EBMBA was in satisfactory agreement. However, our data for COC show that $\phi(T)$ is continuously varying from the pre-transition region into the supercooled region (Figure 2) and goes through a maximum slope in the region of $T_{CT2-CT1}$. Thus the $(T - T^*)^{-\gamma}$ law is not obeyed by COC. Ryumtsev and co-workers[13] studied the optical rotation behavior for cholesteryl butyrate (CBu), cholesteryl palmitate (CP), and cholesteryl nonanoate (CN) in both the isotropic, stable CT1, and supercooled CT1 phases, and found that $\phi(T)$ increased dramatically with decreasing temperature up to a maximum slope condition, followed by a reduced, but *continuous* increase to the lowest temperatures measured in the supercooled phase. Our behavior for $T \simeq T_C$ and for $T > T_C$ for COC is in accord with their observations and so it appears that the $(T - T^*)^{-\gamma}$ relation does not hold for cholesterics as they are cooled from isotropic → CT1 → supercooled CT1 phases. Ryumtsev and co-workers consider that the increase in $\phi(T)$ might possibly be due to the appearance of the CT2 phase as nuclei in the CT1 phase the dimensions of which increase as the temperature is decreased. However, in view of the similarities in behavior for the different cholesterics and the fact that we found our data of Figure 2 to be reversible with temperature and with no apparent discontinuities indicative of a first order transition T_{I-CT1} above $T_{CT2-CT1}$, we suggest that the behavior of $\phi(T)$ for $T > T_C$ and $T < T_C$ is an intrinsic property of an isotropic liquid in which strong angular correlations between molecules develop with decreasing temperature. We suggest that the transition I → CT1 is not a first or second order thermodynamic transition but is approximately at a temperature at which the Bragg reflections first appear giving an optical transition from transparent isotropic phase I to an homeotropic "blue" phase CT1. We suggest that the CT1 phase is a continuation of the isotropic Phase I in the thermodynamic sense, but observe that in the range $T_{CT2-CT1}$ to T_{CT1-I} the angular correlations between molecules build-up rapidly with decreasing temperature leading to a marked variation in the thermodynamic properties of the phase. This means that when $T_{CT2-CT1}$ is reached, the organization within the "blue-phase" is very extensive and if the transition CT2 → CT1 is allowed to occur, by a distinct nucleated process, then only a very small enthalpy change ΔH (and hence entropy change ΔS) will be observed—as is confirmed by Armitage and Price[16,17] and Armitage and Cox.[21] By comparison, the thermodynamic changes observed by differential scanning calorimetry as the isotropic material orders locally on going from I into the CT1 range are relatively much larger—as is confirmed by Armitage and Price[16,17] and Armitage and Cox[21]—and we emphasize that the latter authors observed that the apparent transition CT1 → I is broad, indicative of a second order transition or, in our view, indicative of a marked but continuous variation in the local structure of the isotropic liquid over a narrow range of temperature.

This picture of the isotropic (I) and CT1 phases implies that phases I and CT1 are continuous with each other. Also CT1 for $T < T_{CT2-CT1}$ is the supercooled form of CT1, being continuous in all respects with the phase above this transition temperature. The essential feature is that phases I and CT1 are liquid in the sense that fluctuations occur continually leading to the continual randomization and "break-up" of regions of angularly correlated molecules. X-ray structural investigations of phase CT1 can give little information on the dynamics of phase CT1, but the Kerr-effect data presented here for the phase I and the dynamic light-scattering data for phase I and for CT1 both above and below $T_{CT2-CT1}$ show that motions of the regions of angularly-correlated molecules are rapid and extensive even below $T_{CT2-CT1}$. Thus the phase CT1, although structured on a time-averaged basis, is continually changing its complexions as local regions undergo fluctuations. As T is decreased, the degree of order for phase CT1 increases and when $T_{CT2-CT1}$ is reached, essentially all individual molecules are correlated with their surrounding molecules in a system undergoing continual change. Thus down to $T_{CT2-CT1}$ the Kerr-effect and light-scattering relaxation strengths and correlation times exhibit their most marked increases with decreasing temperature. For $T < T_{CT2-CT1}$ we observe a less rapid increase in the relaxation strengths and correlation times for light-scattering and for $\phi(T)$, showing that the degree of order is now changing less rapidly than was the case in the pre-transition range. Our light-scattering data for COC are in broad agreement with those of Harada and Crooker.[40] They found I_{VV}^{-1} and I_{VH}^{-1} were proportional to $(T - T_a^*)$, with $T_a^* = 304.7$ K for their sample for $T > 305$ K, but for the supercooled range $T < 305$ K these quantities decreased asymptotically to zero with decreasing temperature. The line-widths Γ_{VV} and Γ_{VH} were found to be proportional to $(T - T_\beta^*)$ with $T_\beta^* = 304.3$ K for $T > 305$ K, but for lower temperatures these quantities decreased asymptotically to zero. They found a single Lorentzian fit for $T > 305$ K, but broader curves at lower temperatures, as we have found. Mahler and co-workers[41] also studied COC in the isotropic and CT1 phases using dynamic light scattering. Their data for intensity and line-width variations give different temperature dependencies.

Ryumtsev and co-workers[42] studied the pre-transitional behavior of cholesteryl acetate (CA), cholesteryl nonanoate (CN), cholesteryl propionate (CPr), cholesteryl chloride (CC1), cholesteryl valerate (CV) and cholesteryl octyl carbonate (COctC), using static Kerr-constant measurements. CA, CPr, CV, and CN all had negative Kerr-constants for $T > T_C + 5$ K, but as the temperature was decreased, B first became increasingly negative, reached a minimum value, then varied rapidly and changed sign in the manner analogous to that for $\phi(T)$ in Figure 2. For CC1 and COctC, B was positive throughout the pre-transition region and the behavior was quite similar to that for COC (Figure 2). Ryumtsev and co-workers interpret the negative sign of B for CA, CPr, CV,

and CN and the positive sign of B for CCl and COctC as $T \to \infty$ in terms of the direction of the dipole moment with respect to the axis of maximum polarizability, while the anomalous pre-transitional variation in (T) was interpreted in terms of the emergence of supramolecular formations in the amorphous liquid phase. Our data for COC are consistent with those of Ryumtsev and co-workers.

Finally we note that molecular interpretations of the Kerr-effect and light-scattering data may be approached in terms of molecular theories given by Kielich.[43] For the simple model of N equivalent axially-symmetric molecules, the Kerr-constant is the sum of an induced moment contribution B_{ind} and a dipolar contribution B_μ where

$$B_{\text{ind}} = \frac{4\pi}{45kT} \cdot \Delta\alpha_0 \, \Delta\alpha_\infty \sum_{i=1}^{N} \sum_{j=1}^{N} \frac{\langle 3\cos^2 \theta_{ij} - 1 \rangle}{2} \tag{9a}$$

$$B_\mu = \frac{4\pi\mu^2}{45k^2T^2} \Delta\alpha_\infty \sum_{i=1}^{N} \sum_{j=1}^{N} \sum_{k=1}^{N} \frac{\langle 3\cos\theta_{ij}\cos\theta_{ik} - \cos\theta_{jk} \rangle}{2} \tag{9b}$$

$\Delta\alpha_0$ and $\Delta\alpha_\infty$ refer to the low and high frequency anisotropy of polarizability respectively, and μ is the molecular dipole moment. θ_{ij} is the angle between the major axes of molecules i and j respectively. Thus the magnitude of the Kerr-constant for COC will involve two contributions B_{ind} and B_μ where, for simpler systems, we would expect[44] $B_\mu \gg B_{\text{ind}}$. Both B_{ind} and B_μ comprise auto- and cross-correlation terms for the molecules. The depolarized light-scattering intensity may also, for the simple model system of axially-symmetrical molecules, be related to auto- and cross-correlation terms of the form contained in Eq. 9a (see Refs. 5 and 43). Thus the remarkable increase in B_{obs} and I_{VH} with decreasing temperature may be interpreted as being due to the build-up of angular correlations between molecules, giving substantial contributions to B_{ind} and B_μ. Note that B_μ contains both two-molecule and three-molecule correlation terms, so as the isotropic phase becomes more organized with decreasing temperature, the term B_μ would be expected to vary remarkably—as is observed for COC. The relaxation behavior is more complicated. For B_{ind} the generalization of Eq. 9a to the dynamic case will lead to auto-correlation functions $\langle P_2(\cos\theta_{ii}(t)) \rangle$ and cross-correlation functions, the latter being extremely complicated, but these are defined by Pecora.[45] The generalization of Eq. 9b to the dynamic case will lead to $\langle P_2(\cos\theta_{ii}(t)) \rangle$ for the auto-correlation terms, but the form for the cross-correlation functions has not yet been formulated. In terms of the above approach we conclude that as the temperature of the isotropic liquid is decreased towards T_C the build-up of angular correlations between molecules leads to an increasing contribution from the cross-correlation terms in Eq. 9 (and in the corresponding equation[5,43] for I_{VH}). As

the temperature is decreased through and below T_C the extent of the angular correlations tends to saturate, since the material is now well-organized on average, but with a continually-changing complexion. Thus below T_C, I_{VH} and τ_{VH}, although still increasing with decreasing temperature, do so with a decreasing rate—leading to a maximum in (dI_{VH}/dT) and $(d\tau_{VH}/dT)$—a variation also consistent with the behavior of $\phi(T)$ shown in Figure 1.

Acknowledgments

The authors wish to thank the Science Research Council for the award of research grants to M.S.B. and D.A.E. and for an equipment grant, and Dr. A. H. Price for providing us with the sample of COC. The authors wish to express their thanks to Dr. P. Pusey of R.S.R.E. Malvern for his collaboration in the quasi-elastic light-scattering experiments.

References

1. J. D. Litster and T. W. Stinson, *J. Appl. Phys.*, **41**, 996 (1970).
2. T. W. Stinson and J. D. Litster, *Phys. Rev. Lett.*, **25**, 503 (1970).
3. M. S. Beevers, *Mol. Cryst. Liq. Cryst.*, **31**, 333 (1975).
4. H. J. Coles and B. R. Jennings, *Molec. Phys.*, **31**, 571, 1225 (1976).
5. T. D. Gierke and W. H. Flygare, *J. Chem. Phys.*, **61**, 2231 (1974).
6. M. Davies, R. Moutran, A. H. Price, M. S. Beevers and G. Williams, *J. Chem. Soc., Faraday II*, **72**, 1447 (1976).
7. H. J. Coles and B. R. Jennings, *Molec. Phys.*, **36**, 1661 (1978).
8. M. Schadt, *J. Chem. Phys.*, **67**, 210 (1977).
9. P. G. de Gennes, *Mol. Cryst. Liq. Cryst.*, **12**, 193 (1971).
10. P. G. de Gennes, *'The Physics of Liquid Crystals'*, Oxford University Press (1974).
11. G. W. Gray, *'Molecular Structure and the Properties of Liquid Crystals'*, Academic Press, New York (1962).
12. D. Coates and G. W. Gray, *Phys. Lett.*, **45A**, 115 (1973).
13. E. I. Ryumtsev, A. N. Cherkasov, V. G. Tischenko and M. M. Fetisova, *Sov. Phys. Crystallogr.*, **18**, 657 (1974).
14(a) F. P. Price and J. H. Wendorff, *J. Phys. Chem.*, **75**, 2839 (1971).
(b) F. P. Price and J. H. Wendorff, *J. Phys. Chem.*, **76**, 276 (1972).
15. H. Stegemeyer and K. Bergmann, in *'Liquid Crystals of One and Two Dimensional Order'* (eds. W. Helfrich and G. Heppke), Springer Series in Chem. Physics, 11, 1980, p. 161.
16. D. Armitage and F. P. Price, *J. Appl. Phys.*, **47**, 2735 (1976).
17. D. Armitage and F. P. Price, *J. Chem. Phys.*, **66**, 3414 (1977).
18. P. J. Collins and J. R. McColl, *J. Chem. Phys.*, **69**, 3371 (1978).
19. S. A. Jabarin and R. S. Stein, *J. Phys. Chem.*, **77**, 399 (1973).
20. T. Asada, *Kyoto Daigaku Nippon Kagakimesi Kenkyusho Koenshu*, **31**, 1 (1974).
21. D. Armitage and R. J. Cox, *Mol. Cryst. Liq. Cryst. Lett.*, **64**, 41 (1980).
22. I. G. Chistyakov and L. A. Gusakova, *Sov. Phys. Crystallogr.*, **14**, 132 (1969).
23. W. Elser, J. L. W. Pohlemann and P. R. Boyd, *Mol. Cryst. Liq. Cryst.*, **20**, 77, 87 (1973).
24. A. Saupe, *Mol. Cryst. Liq. Cryst.*, **7**, 59 (1969).
25. D. A. Elliott, Ph.D. Thesis, Univ. of Wales, 1980.
26. M. S. Beevers and D. A. Elliott, *Mol. Cryst. Liq. Cryst.*, **53**, 111 (1979).
27. H. Watanabe in *'Electro-optics and Dielectrics of Macromolecules and Colloids'* (ed. B. R. Jennings), Plenum Press, New York, 1979, p. 43.
28. J. Cheng and R. B. Meyer, *Phys. Rev. Lett.*, **29**, 1240 (1972).
29. J. Cheng and R. B. Meyer, *Phys. Rev.*, **A9**, 2744 (1974).
30. M. Evans, R. Moutran and A. H. Price, *J. Chem. Soc., Faraday II*, **71**, 1854 (1975).

31. G. W. Gray and M. Hannant, *Mol. Cryst. Liq. Cryst., Lett.*, **53**, 263 (1979).
32. M. S. Beevers, J. Crossley, D. C. Garrington and G. Williams, *J. Chem. Soc., Faraday II*, **73**, 458 (1977).
33. J. Crossley, D. A. Elliott and G. Williams, *J. Chem. Soc., Faraday II*, **75**, 88 (1979).
34. M. S. Beevers, D. A. Elliott and G. Williams, *Polymer*, **21**, 13 (1980).
35. H. Z. Cummins and E. R. Pike, *'Photon Correlation and Light-beating Spectroscopy'*, Plenum Press, New York, 1974.
36. P. N. Pusey and J. M. Vaughan, in *'Dielectric and Related Molecular Processes'* (ed. M. Davies), Chem. Soc. Spec. Period. Reports, **2**, 48 (1975).
37. G. Williams and D. C. Watts, *Trans. Faraday Soc.*, **66**, 80 (1970).
38. G. Williams, D. C. Watts, S. B. Dev and A. M. North, *Trans. Faraday Soc.*, **67**, 1323 (1971).
39. C. C. Yang, *Phys. Rev. Lett.*, **28**, 955 (1972).
40. T. Harada and P. P. Crooker, *Phys. Rev. Lett.*, **34**, 1259 (1975).
41. D. S. Mahler, P. H. Keyes and W. B. Daniels, *Phys. Rev. Lett.*, **36**, 491 (1976).
42. E. I. Ryumtsev, M. V. Mukhina and V. N. Tsvetkov, *Dokl. Akad. Nauk SSR*, **204**, 397 (1972).
43. S. Kielich in *'Dielectric and Related Molecular Processes'* (ed. M. Davies), Specialist Periodical Reports, The Chemical Society, London, Vol. 2, 1972, p. 192.
44. H. A. Stuart, *'Molecülstructur'*, 3rd Edition, Springer-Verlag, Berlin, 1967.
45. R. Pecora, *J. Chem. Phys.*, **50**, 2650 (1968).

Appendix

In view of their complicated transition behavior, there exists some confusion in the use of the term "T_c" for cholesteric materials. Price and Wendorff[14] called their T_{CT1-I} the temperature of the "cholesteric-isotropic transition." Many authors regard the state CT1 as being a form of the cholesteric state.[11,12,14] The isotropic liquid shows remarkable pretransitional behavior due to the formation of chiral structures (whose position and composition fluctuate in time as is evidenced by this and earlier studies); thus the term "isotropic liquid" requires careful consideration for cholesterics (and nematics). In the work of de Gennes[9,10] and Cheng and Meyer[28,29] it is implicit that T^*, which relates to the *pre*-transitional behavior, obeys the relation $T^* \leqslant T_c$. For COC, Harada and Crooker say that the cholesteric texture is observed "below about $T_c = 31°C$, at which point it undergoes a first order phase transition to the textureless isotropic phase." In the range 28.5 to 31.5°C a supercooled metastable isotropic phase could be obtained. Their light scattering data yield, from the high temperature results, a T^* value of 31.5°C, being greater than the quoted T_c value. The same result in $T^* > T_c$ is obtained from extrapolation of the high-temperature data of Mahler *et al.* for the line-width Γ, but a different extrapolation value having $T^* = T_c$ is obtained from their intensity data. As will be seen in the present work, extrapolations of light-scattering data do not yield an unambiguous T^* value.

On heating, the CT2 material (see Figure 1) the transition CT2 → CT1 occurs giving a marked optical change from white-opaque to transparent-homeotropic. As the temperature is further raised, the material transforms

over a range so that at T_{CT1-I} it appears wholly isotropic. Such changes are discussed in the text. In order to avoid confusion we do not use the term "T_c," but $T_{CT2-CT1}$ or T_{CT1-I} dependent upon the transformation being considered. We stress that the CT1 material may be supercooled to below $T_{CT2-CT1}$ and our data for $\phi(T)$, $I_{VV}(T)$, $I_{VH}(T)$ and the correlation times $\tau_{VV}(T)$ and $\tau_{VH}(T)$ for $T < T_{CT2-CT1}$ all refer to the supercooled CT1 material (i.e., homeotropic material).